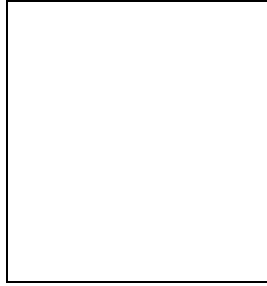


Supersymmetric Lepton Flavor Violation and Leptogenesis

S. Albino^a, F. Deppisch^b, R. Rückl^a

^a*Institut für Theoretische Physik und Astrophysik, Universität Würzburg, D-97074 Würzburg, Germany*

^b*Deutsches Elektronen-Synchrotron DESY, D-22603 Hamburg, Germany*



We present and discuss constraints on supersymmetric type I seesaw models imposed by neutrino data, charged lepton flavor violation and thermal leptogenesis.

1 Supersymmetric seesaw mechanism and slepton mass matrix

The observed neutrino oscillations imply the existence of neutrino masses and lepton flavor mixing, and give hints towards physics beyond the Standard Model. For example, the smallness of the neutrino masses suggests the realization of the seesaw mechanism involving heavy right-handed Majorana neutrinos. The latter violate lepton number and CP , and thus allow for leptogenesis. Particularly interesting are supersymmetric scenarios, where the lepton flavor violation (LFV) present in the neutrino sector is transmitted to the slepton sector giving also rise to measurable LFV processes of charged leptons.

A minimal model of this kind is obtained if three right-handed neutrino singlet fields ν_R are added to the MSSM particle content. In this model, one can have the following Majorana mass and Yukawa interaction terms¹:

$$-\frac{1}{2}\nu_R^{cT} M \nu_R^c + \nu_R^{cT} Y_\nu L \cdot H_2, \quad (1)$$

where M is the Majorana mass matrix, Y_ν is the matrix of Yukawa couplings, and L and H_2 denote the left-handed lepton and hypercharge $+1/2$ Higgs doublets, respectively. Electroweak symmetry breaking then generates the neutrino Dirac mass matrix $m_D = Y_\nu \langle H_2^0 \rangle$ where $\langle H_2^0 \rangle = v \sin \beta$ is the appropriate Higgs v.e.v. with $v = 174$ GeV and $\tan \beta = \frac{\langle H_2^0 \rangle}{\langle H_1^0 \rangle}$. If the mass scale M_R of the matrix M is much greater than the electroweak scale, and thus much greater than the scale of m_D , one naturally obtains three light neutrinos with the mass matrix

$$M_\nu = m_D^T M^{-1} m_D = Y_\nu^T M^{-1} Y_\nu (v \sin \beta)^2, \quad (2)$$

and three heavy neutrinos with the mass matrix $M_N = M$. In the basis assumed, M is diagonal, while M_ν is to be diagonalized by the unitary MNS matrix U :

$$\begin{aligned} U^T M_\nu U &= \text{diag}(m_1, m_2, m_3), \\ U &= V_{\text{CKM}}(\theta_{12}, \theta_{13}, \theta_{23}, \delta) \cdot \text{diag}(e^{i\phi_1}, e^{i\phi_2}, 1), \end{aligned} \quad (3)$$

θ_{ij} being mixing angles, δ and ϕ_i being Dirac and Majorana phases, respectively, and m_i being the light neutrino mass eigenvalues.

The heavy neutrino mass eigenstates N , which are too heavy to be observed directly, influence the evolution of the MSSM slepton mass matrix:

$$m_{\tilde{l}}^2 = \begin{pmatrix} m_L^2 & m_{LR}^{2\dagger} \\ m_{LR}^2 & m_R^2 \end{pmatrix}_{\text{MSSM}} + \begin{pmatrix} \delta m_L^2 & \delta m_{LR}^{2\dagger} \\ \delta m_{LR}^2 & \delta m_R^2 \end{pmatrix}_N. \quad (4)$$

It is these flavor off-diagonal virtual effects which lead to charged LFV. Adopting the minimal supergravity (mSUGRA) scheme one finds, in leading logarithmic approximation²,

$$\delta m_L^2 = -\frac{1}{8\pi^2}(3m_0^2 + A_0^2)Y_\nu^\dagger L Y_\nu, \quad \delta m_R^2 = 0, \quad \delta m_{LR}^2 = -\frac{3}{16\pi^2}A_0 v \cos \beta Y_l Y_\nu^\dagger L Y_\nu, \quad (5)$$

where $L_{ij} = \ln(M_{\text{GUT}}/M_i)\delta_{ij}$, M_i being the heavy neutrino masses, and m_0 and A_0 are the universal scalar mass and trilinear coupling, respectively, at the GUT scale M_{GUT} .

By inverting (2), the neutrino Yukawa matrix can be written as follows¹:

$$Y_\nu = \frac{1}{v \sin \beta} \text{diag}(\sqrt{M_1}, \sqrt{M_2}, \sqrt{M_3}) \cdot R \cdot \text{diag}(\sqrt{m_1}, \sqrt{m_2}, \sqrt{m_3}) \cdot U^\dagger. \quad (6)$$

Here, a new complex orthogonal matrix R appears which may be parametrized in terms of 3 complex angles $\theta_i = x_i + iy_i$:

$$R = \begin{pmatrix} c_2 c_3 & -c_1 s_3 - s_1 s_2 c_3 & s_1 s_3 - c_1 s_2 c_3 \\ c_2 s_3 & c_1 c_3 - s_1 s_2 s_3 & -s_1 c_3 - c_1 s_2 s_3 \\ s_2 & s_1 c_2 & c_1 c_2 \end{pmatrix}, \quad (7)$$

with $(c_i, s_i) = (\cos \theta_i, \sin \theta_i) = (\cos x_i \cosh y_i - i \sin x_i \sinh y_i, \sin x_i \cosh y_i + i \cos x_i \sinh y_i)$. While the light neutrino masses m_i and the mixing angles θ_{ij} have been measured or at least constrained, the phases ϕ_i and δ , the heavy neutrino masses M_i and the matrix R are presently unknown. Using the available neutrino data³ as input in the appropriate renormalization group equations, Y_ν is evolved from the electroweak scale to the GUT scale and then put into the renormalization of the slepton mass matrix from M_{GUT} to the electroweak scale.

2 Charged lepton flavor violation

The renormalization effects (5) lead to charged LFV either via contributions of virtual sleptons in loops such as in radiative decays $l_i \rightarrow l_j \gamma$, or via real slepton production and decay such as in $e^+ e^- \rightarrow \tilde{l}_a^- \tilde{l}_b^+ \rightarrow l_i^- l_j^+ + 2\tilde{\chi}_1^0$. To lowest order in LFV couplings one has^{1,2}

$$\Gamma(l_i \rightarrow l_j \gamma) \propto \alpha^3 m_{\tilde{l}_i}^5 \frac{|(\delta m_L)_{ij}^2|^2}{\tilde{m}^8} \tan^2 \beta, \quad (8)$$

\tilde{m} characterizing the typical sparticle masses in the loop. Similarly, one finds⁴

$$\sigma(e^+ e^- \rightarrow l_i^- l_j^+ + 2\tilde{\chi}_1^0) \approx \frac{|(\delta m_L)_{ij}^2|^2}{m_{\tilde{l}_i}^2 \Gamma_{\tilde{l}_i}^2} \sigma(e^+ e^- \rightarrow l_i^- l_i^+ + 2\tilde{\chi}_1^0). \quad (9)$$

Consequently, light neutrino data imply interesting constraints on LFV processes through the dependence on $|(Y_\nu^\dagger LY_\nu)_{ij}|^2$ with Y_ν given by Eq. (6). Conversely, measurements or bounds on LFV processes can constrain the fundamental seesaw parameters M_i and R .

For simplicity, we first consider the case of mass degenerate heavy Majorana neutrinos with $M_i = M_R$. If R is real, i.e. $y_i = 0$, then it will drop out from the product $Y_\nu^\dagger Y_\nu$ in this case as do the Majorana phases ϕ_1 and ϕ_2 , leaving M_R and δ as the only unconstrained parameters. Fig. 1a shows the typical rise of $\text{Br}(l_i \rightarrow l_j \gamma)$ with M_R^2 suggested by Eq. (8) for fixed light neutrino masses. Also shown is the impact of the uncertainties in the neutrino data. From the present bound⁵ $\text{Br}(\mu \rightarrow e \gamma) < 1.2 \cdot 10^{-11}$ one can derive an upper limit on M_R of order 10^{14} GeV. Furthermore, from Eqs. (8) and (9) the uncertainties in the neutrino parameters are expected to drop out of the correlation of radiative decays and scattering processes in the same LFV channel. This is demonstrated in Fig. 1b for the $\tau\mu$ channel. As can be seen, combined measurements of both processes provide decisive tests of the considered scenarios.

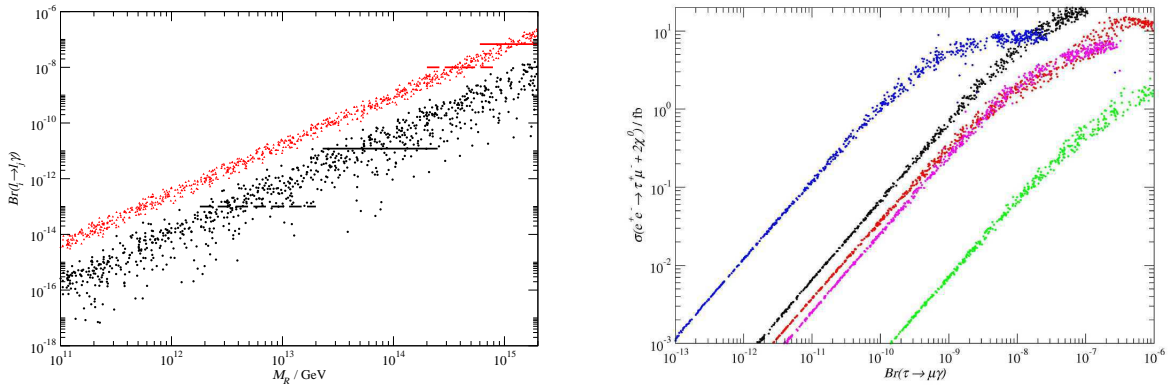


Figure 1: (a) $\text{Br}(\tau \rightarrow \mu \gamma)$ (upper points) and $\text{Br}(\mu \rightarrow e \gamma)$ (lower) versus M_R in mSUGRA scenario SPS1a for real R . The light neutrino masses are assumed quasi-degenerate. The mixing angles and the Dirac phase are scattered within the full ranges consistent with experiment. The solid (dashed) horizontal lines mark the present^{6,5} (expected future) bounds, $\text{Br}(\tau \rightarrow \mu \gamma) < 6.8 \times 10^{-8}$ (10^{-8}) and $\text{Br}(\mu \rightarrow e \gamma) < 1.2 \times 10^{-11}$ (10^{-13}). (From⁷.) (b) $\sigma(e^+e^- \rightarrow \tau^+\mu^- + 2\tilde{\chi}_1^0)$ versus $\text{Br}(\tau \rightarrow \mu \gamma)$. The light neutrino parameters are scattered as in (a). The plots (from left to right) are calculated in the mSUGRA scenarios C', B', SPS1a, G' and I'. (From⁴.)

The above results are rather conservative, since LFV processes will be enhanced if the light neutrino masses are hierarchical instead of degenerate, and/or if R is complex. In the latter case, LFV observables have rather more freedom since the dependence on the y_i can be as significant as the M_R dependence, as Fig. 2 shows. The change in $Y_\nu^\dagger Y_\nu$ is approximately

$$\Delta_R(Y_\nu^\dagger Y_\nu) \approx U \text{diag}(\sqrt{m_i})(R^\dagger R - \mathbf{1}) \text{diag}(\sqrt{m_i})U^\dagger. \quad (10)$$

Eq. (10) implies two features seen in Fig. 2: (i) Compared to the case of degenerate light neutrino masses, the y dependence in the hierarchical case is weaker since the condition $m_3 \gg m_{1,2}$ implies that only $(R^\dagger R - \mathbf{1})_{33} = O(y_i^2)$ contributes. (ii) Since Eq. (10) is approximately imaginary and linear in the y_i , non-zero y_i can only increase the observable so that lower limits obtained for real R remain unaffected. Even small values of y can enhance a process by orders of magnitude from the real R result. Also, in contrast to the real R case, the LFV branching ratios for degenerate neutrinos can now be larger than that for hierarchical neutrinos.

3 Leptogenesis

In thermal leptogenesis the baryon asymmetry of the universe is generated from out-of-equilibrium decays of the heavy Majorana neutrinos (see e.g.^{8,9}). Most models are based on the assumption of a hierarchical mass spectrum $M_1 \ll M_2 \ll M_3$. It is then natural to assume that light

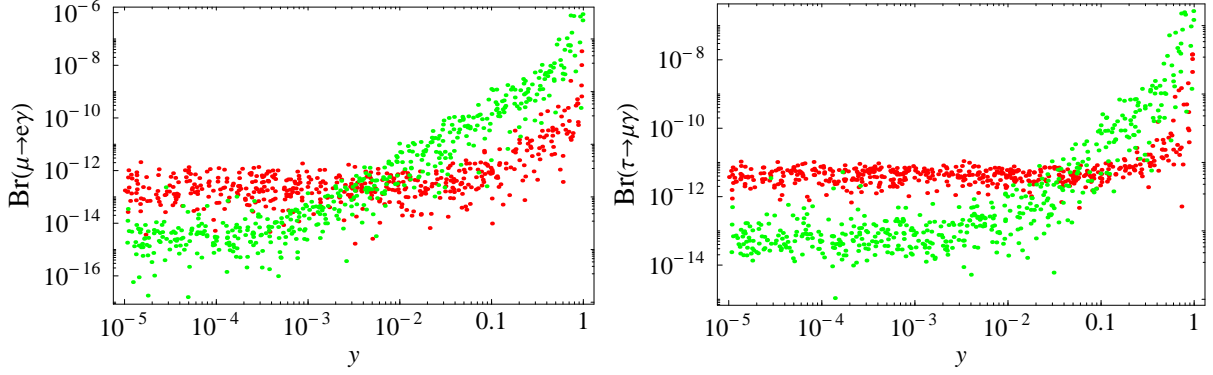


Figure 2: $\text{Br}(l_i \rightarrow l_j \gamma)$ versus $y_i = y$ for fixed $M_R = 10^{12}$ GeV in mSUGRA scenario SPS1a for hierarchical (dark points) and degenerate (light) light neutrino masses. The parameters are scattered as in Fig. 1a. In addition, the x_i are scattered over their full range $0 < x_i < 2\pi$.

neutrino masses are also hierarchical. In this case, the baryon to photon ratio is determined by four factors which are briefly explained below:

$$\eta_B \equiv \frac{n_B - n_{\bar{B}}}{n_\gamma} \approx d a_{\text{Sph}} \epsilon_1 \kappa_f. \quad (11)$$

The CP asymmetry ϵ_1 generated in the decays of the lightest of the heavy Majorana neutrinos N_1 is^{10,11}

$$\epsilon_1 \equiv \frac{\Gamma(N_1 \rightarrow h_2 + l) - \Gamma(N_1 \rightarrow \bar{h}_2 + \bar{l})}{\Gamma(N_1 \rightarrow h_2 + l) + \Gamma(N_1 \rightarrow \bar{h}_2 + \bar{l})} \approx -\frac{3}{8\pi} \frac{M_1}{v^2 \sin^2 \beta} \frac{\sum_i m_i^2 \text{Im}(R_{1i}^2)}{\sum_i m_i |R_{1i}|^2}. \quad (12)$$

This relation clearly shows that non-zero imaginary parts of the R matrix elements are necessary to generate a CP asymmetry. The efficiency factor κ_f in (11) takes into account the washout of the initial $(B - L)$ asymmetry. A reliable numerical fit for κ_f for hierarchical light neutrinos in the strong washout regime can be found in⁸. The solar and atmospheric neutrino mass fits favor a value $\kappa_f = \mathcal{O}(10^{-2})$. The $(B - L)$ asymmetry is subsequently converted to a baryon asymmetry by sphaleron processes. In the case of the MSSM one obtains the conversion factor $a_{\text{Sph}} = \frac{8}{23}$. Finally, one has to take into account the dilution of the asymmetry due to standard photon production, described by the dilution factor $d \approx \frac{1}{78}$ in the MSSM. Confronted with the observed baryon asymmetry¹² $\eta_B = (6.3 \pm 0.3) \cdot 10^{-10}$, relation (12) implies a lower bound on the M_1 scale¹¹, e.g. if $\epsilon_1 > 10^{-6}$, then $M_1 > 4 \cdot 10^9$ GeV. Furthermore, to allow for thermal production of right-handed neutrinos after inflation, we require $M_1 < 10^{11}$ GeV, the maximum order of magnitude that the reheating temperature can reach without suffering an overabundance of gravitinos, whose decay into energetic photons can otherwise spoil big bang nucleosynthesis. In the above mass range, the condition to reproduce the experimental baryon asymmetry then puts constraints on the parameters x_2 and x_3 of the R matrix¹³ as illustrated in Fig. 3a. With decreasing $M_1 < 10^{11}$ GeV, the allowed values for x_2 are concentrated more and more at $\sin x_2 = 0$. A similar behaviour is found for the angle x_3 .

As discussed in the previous section for degenerate Majorana neutrinos, experimental limits on $\text{Br}(\mu \rightarrow e \gamma)$ can be used to constrain the heavy neutrino scale, here represented by the heaviest Majorana neutrino mass M_3 . This is shown in Fig. 3b. The present bound on $\text{Br}(\mu \rightarrow e \gamma)$ constrains M_3 already to be smaller than 10^{13} GeV. Future experiments are expected to reach below $M_3 = 10^{12}$ GeV.

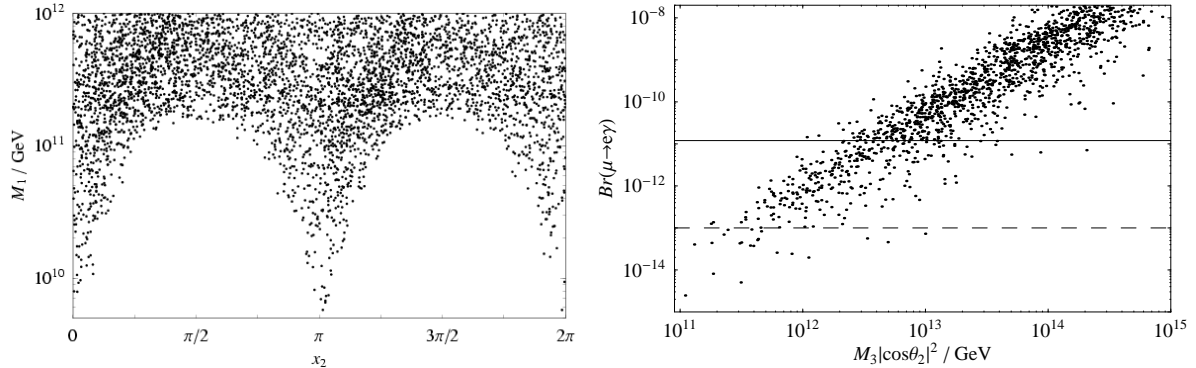


Figure 3: (a) Region in the plane (x_2, M_1) consistent with the generation of the baryon asymmetry $\eta_B = (6.3 \pm 0.3) \cdot 10^{-10}$ via leptogenesis. (b) $Br(\mu \rightarrow e\gamma)$ as a function of M_3 in mSUGRA scenario SPS1a, for $M_1 = 10^{10}$ GeV. The solid (dashed) line indicates the present (expected future) experimental sensitivity. All other seesaw parameters are scattered in their allowed ranges for hierarchical light and heavy neutrinos.

4 Concluding remarks

Supersymmetric LFV is very model dependent. As far as the mSUGRA parameters are concerned, this is further emphasized in Fig. 4, where a scan in the $(m_0, m_{1/2})$ plane is performed showing contours of fixed LFV cross section at the ILC and $\mu \rightarrow e\gamma$ branching ratio. Clearly, the strategy to probe LFV considered here will only be applicable once sufficient measurements of the SUSY particles' properties have been made.

In a given scenario LFV observables, particularly in the μe channel, are very sensitive to uncertainties in the neutrino parameters. However, correlations of observables in the same LFV channel suffer much less from this. As demonstrated in Fig. 1b, such correlations can be rather strong, and therefore very useful probes. Although less pronounced, relations also exist among observables in different LFV channels like $\tau\mu$ and μe . These can be exploited to improve direct bounds. Fig. 5 illustrates this for a variety of seesaw parameters, uncovering a rather good correlation between the μe and $\tau\mu$ channels. One sees that the present experimental bound on $Br(\mu \rightarrow e\gamma)$ can be used to improve the direct bound on $Br(\tau \rightarrow \mu\gamma)$ by almost 2 orders of magnitude. Interestingly, this result does not depend on whether hierarchical or degenerate heavy and light neutrinos are assumed.

For hierarchical Majorana masses, leptogenesis provides additional constraints. For a heavy Majorana neutrino mass spectrum obeying 10^{10} GeV $\approx M_1 \ll M_2 \ll M_3 \approx 10^{13}$ GeV (in mSUGRA scenario SPS1a), both LFV and leptogenesis are found to be viable. The heaviest Majorana mass M_3 is constrained from above by the LFV process $\mu \rightarrow e\gamma$, the lightest mass M_1 from below by leptogenesis. In addition, the orthogonal R matrix encoding the mixing of the right-handed neutrinos, which is parametrized by the angles $\theta_i = x_i + iy_i$, is constrained according to $\sin x_{2,3} \simeq 0$ and $y_i < \mathcal{O}(1)$ as a consequence of the successful leptogenesis condition for small M_1 and the requirement of perturbative Yukawa couplings, respectively. Finally, the remaining parameter x_1 can be constrained from the ratio $Br(\mu \rightarrow e\gamma)/Br(\tau \rightarrow \mu\gamma)$ ¹³. Other work along this line can be found in the literature (for references see¹³) and has also been presented at this meeting (see e.g.¹⁴).

Acknowledgments

We thank H. Päs, A. Redelbach and Y. Shimizu for fruitful collaboration. This work was supported by the Federal Ministry of Education and Research (BMBF) under contract number 05HT1WWA2.

Figure 4: Contours of the polarized cross section $\sigma(e^+e^- \rightarrow \mu^+e^- + 2\tilde{\chi}_1^0)$ at $\sqrt{s}_{ee} = 800$ GeV in the $m_0 - m_{1/2}$ plane (solid lines). The remaining mSUGRA parameters are: $A_0 = 0$ GeV, $\tan\beta = 5$, $\text{sign}(\mu) = +$. The beam polarizations are: $P_{e^-} = +0.9$, $P_{e^+} = +0.7$. For comparison, $\text{Br}(\mu \rightarrow e\gamma)$ is shown by dashed lines. The neutrino oscillation parameters are fixed at their best fit values, the lightest neutrino mass and all complex phases are set to zero, and the degenerate Majorana mass scale is $M_R = 10^{14}$ GeV. The shaded (red) areas are forbidden by mass bounds from various experimental sparticle searches.

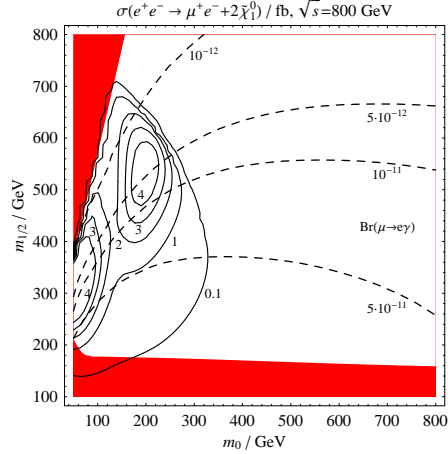
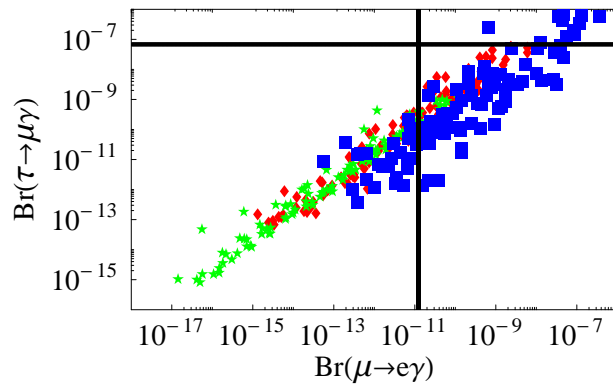


Figure 5: $\text{Br}(\tau \rightarrow \mu\gamma)$ versus $\text{Br}(\mu \rightarrow e\gamma)$ in mSUGRA scenario SPS1a, assuming degenerate Majorana masses and hierarchical (diamonds) and degenerate (stars) light neutrino masses, with parameters scattered as in Fig. 1. In the case of hierarchical Majorana and light neutrino masses (squares) all seesaw parameters including the x_i are scattered within their experimentally allowed ranges, while the y_i and M_i are scattered within the bounds demanded by leptogenesis and perturbativity. Also indicated are the present experimental bounds ^{5,6}.



References

1. J. A. Casas and A. Ibarra, Nucl. Phys. B **618**, 171 (2001) [arXiv:hep-ph/0103065].
2. J. Hisano and D. Nomura, Phys. Rev. D **59**, 116005 (1999) [arXiv:hep-ph/9810479].
3. M. Maltoni, T. Schwetz, M.A. Tortola and J.W.F. Valle, Phys. Rev. D **68**, 113010 (2003) [arXiv:hep-ph/0309130].
4. F. Deppisch, H. Päs, A. Redelbach, R. Rückl and Y. Shimizu, Phys. Rev. D **69**, 054014 (2004) [arXiv:hep-ph/0310053].
5. S. Eidelman *et al.* [PDG Collab.], Phys. Lett. B **592**, 1 (2004) [arXiv:hep-ph/0310053].
6. B. Aubert *et al.* [BABAR Collab.], Phys. Rev. Lett. **95**, 041802 (2005) [arXiv:hep-ex/0502032].
7. F. Deppisch, H. Päs, A. Redelbach, R. Rückl and Y. Shimizu, Eur. Phys. J. C **28**, 365 (2003) [arXiv:hep-ph/0206122].
8. W. Buchmüller, P. Di Bari and M. Plümacher, arXiv:hep-ph/0401240.
9. P. Di Bari, arXiv:hep-ph/0406115; P. Di Bari, Nucl. Phys. B **727**, 318 (2005) [arXiv:hep-ph/0502082].
10. M. Plümacher, arXiv:hep-ph/9807557 and references therein.
11. S. Davidson and A. Ibarra, Phys. Lett. B **535**, 25 (2002) [arXiv:hep-ph/0202239].
12. D. N. Spergel *et al.* [WMAP Collab.], Astrophys. J. Suppl. **148**, 175 (2003) [arXiv:astro-ph/0302209]; M. Tegmark *et al.* [SDSS Collab.], Phys. Rev. D **69**, 103501 (2004) [arXiv:astro-ph/0310723].
13. F. Deppisch, H. Päs, A. Redelbach and R. Rückl, Phys. Rev. D **73**, 033004 (2006) [arXiv:hep-ph/0511062].
14. S.T. Petcov, W. Rodejohann, T. Shindou and Y. Takanishi, Nucl. Phys. B **739**, 208 (2006) [arXiv:hep-ph/0510404]; S.T. Petcov and T. Shindou, [arXiv:hep-ph/0605204].